Deuterated TEKPol Biradicals and the Spin-Diffusion Barrier in MAS DNP

Venkatesh, Amrit; Casano, Gilles; Rao, Yu; De Biasi, Federico; Perras, Frédéric A.; Kubicki, Dominik J.; Siri, Didier; Abel, Sébastien; Karoui, Hakim; Yulikov, Maxim; Ouari, Olivier; Emsley, Lyndon

DOI:
10.1002/ange.202304844

Zitierweise: *Angew. Chem. Int. Ed.* **2023**, e202304844
doi.org/10.1002/anie.202304844

NMR Spectroscopy

Deuterated TEKPol Biradicals and the Spin-Diffusion Barrier in MAS DNP

Amrit Venkatesh, Gilles Casano, Yu Rao, Federico De Biasi, Frédéric A. Perras, Dominik J. Kubicki, Didier Siri, Sébastien Abel, Hakim Karoui, Maxim Yulikov, Olivier Ouari, and Lyndon Emsley**

Abstract: The sensitivity of NMR spectroscopy is considerably enhanced by dynamic nuclear polarization (DNP). In DNP polarization is transferred from unpaired electrons of a polarizing agent to nearby proton spins. In solids, this transfer is followed by the transport of hyperpolarization to the bulk via ^{1}H-^{1}H spin diffusion. The efficiency of these steps is critical to obtain high sensitivity gains, but the pathways for polarization transfer in the region near the unpaired electron spins are unclear. Here we report a series of seven deuterated and one fluorinated TEKPol biradicals to probe the effect of deprotonation on MAS DNP at 9.4 T. The experimental results are interpreted with numerical simulations, and our findings support that strong hyperfine couplings to nearby protons determine high transfer rates across the spin diffusion barrier to achieve short build-up times and high enhancements. Specifically, ^{1}H DNP build-up times increase substantially with TEKPol isotopologues that have fewer hydrogen atoms in the phenyl rings, suggesting that these protons play a crucial role transferring the polarization to the bulk. Based on this new understanding, we have designed a new biradical, NaphPol, which yields significantly increased NMR sensitivity, making it the best performing DNP polarizing agent in organic solvents to date.

Introduction

Dynamic nuclear polarization (DNP) considerably improves nuclear magnetic resonance (NMR) spectroscopy by providing 1–2 orders of magnitude in signal enhancement.[1] Magic angle spinning (MAS) DNP is typically performed at high magnetic fields (9.4–21.1 T)[2] by impregnating solids with a solution containing a biradical polarizing agent,[3] or by dissolving the analyte in the radical solution.[4] By far, the most successful DNP experiments to date are performed with nitroxide-containing biradicals[5] such as TEKPol,[6] AMUPol,[7] HydroPol,[8] AsymPols,[9] and TinyPols[10] that enable DNP via the cross effect,[11] a process involving at least two electron spins and one nuclear spin. Efficient DNP has been observed using cross-effect biradicals that possess fixed electron-electron *g*-tensor orientations and distances,[12] long electron relaxation times induced by rigid and bulky functional groups,[6,13] balanced interelectronic couplings,[14] and open conformations.[8] Shorter inter-electronic distances[9a] and hybrid biradicals obtained by tethering nitroxide radicals with narrow-line radicals such as BDPA (as in HyTEK-2)[2b,15] or Trityl (as in TEMTriPol)[2c,16] have yielded improved enhancements at fields above 9.4 T, and have been linked to faster DNP build-up rates.[17] Although the current state-of-the-art biradicals provide high ^{1}H signal enhancements, the highest enhancement (ε) shown to date in bulk solutions at standard DNP conditions of ca. 100 K has only reached roughly a half of the theoretical maximum of 658, with HydroPol yielding $\varepsilon = 330$ at 9.4 T.[8] Enabling high DNP enhancements while

[*] A. Venkatesh, Y. Rao, F. De Biasi, D. J. Kubicki, L. Emsley
Institut des Sciences et Ingénierie Chimiques, Ecole Polytechnique Fédérale de Lausanne (EPFL)
1015 Lausanne (Switzerland)
E-mail: lyndon.emsley@epfl.ch

G. Casano, D. Siri, S. Abel, H. Karoui, O. Ouari
Aix Marseille Université, CNRS, Institut de Chimie Radicalaire, UMR 7273
13013 Marseille (France)
E-mail: olivier.ouari@univ-amu.fr

F. A. Perras
Chemical and Biological Sciences Division, Ames National Laboratory
Ames, IA-50011 (USA)
and
Department of Chemistry, Iowa State University
Ames, IA-5011 (USA)

M. Yulikov
Laboratory of Physical Chemistry, Department of Chemistry, ETH Zürich
8093 Zürich (Switzerland)

D. J. Kubicki
Current address: School of Chemistry, University of Birmingham
Edgbaston B15 2TT (UK)

diminishing depolarization,[18] quenching effects[19] and reducing DNP build-up times will result in higher overall sensitivity gains and therefore open up hitherto unexplored applications of NMR that are sensitivity limited. Consequently, there is much interest in improving the design of DNP polarizing agents.

A critical step in the rational design of optimal and diverse polarizing agents is the development of principles that unambiguously link the molecular structure of biradicals to the DNP efficiency.[20] To achieve this target, a fundamental understanding of the dynamics of the polarization transfer from the electrons to nearby protons, within the so-called spin diffusion barrier (ca. 1 nm radius from the electron), must be developed.[21] Understanding the efficiency of transfer in this first step is crucial as the polarization generated on such nearby protons is then relayed to the bulk sample via ^{1}H-^{1}H spin diffusion.[22] Early on, Wolfe established contact of the spins within 0.3 nm of the radical with the bulk sample,[23] and more recently the spin diffusion barrier was studied using thermodynamic models,[22b] electron paramagnetic resonance (EPR) spectroscopy,[24] microwave-gating[25] and electron decoupling.[26] These observations question the nature of the nuclear spin diffusion barrier and the role of the protons near the electrons in the spin diffusion process and build-up of nuclear hyperpolarization in the bulk.

Selective deuteration of the radicals is a promising approach to unravel such DNP processes. For example, this strategy was used to link the protons involved in Overhauser effect DNP.[27] The effect of deuteration on cross effect biradicals was also previously studied, although a general relationship between deuteration and DNP performance in cross-effect biradicals has not been identified so far.[20,28] Here, we synthesized a series of seven deuterated, and one fluorinated, TEKPol biradicals to study the effect of selective deprotonation on the DNP efficiency at 9.4 T and establish the pathways for polarization transfer across the spin diffusion barrier.

Results and Discussion

Figure 1A shows the structures of the eight new TEKPol biradicals synthesized and studied in this work, where the positions of deuteration and fluorination are highlighted in blue and purple, respectively. Note that there are two sets of radicals where eight (TEKPol-d_8/-d_{8c}) or sixteen protons (TEKPol-d_{16}/-d_{16c}) are replaced with deuterons at different

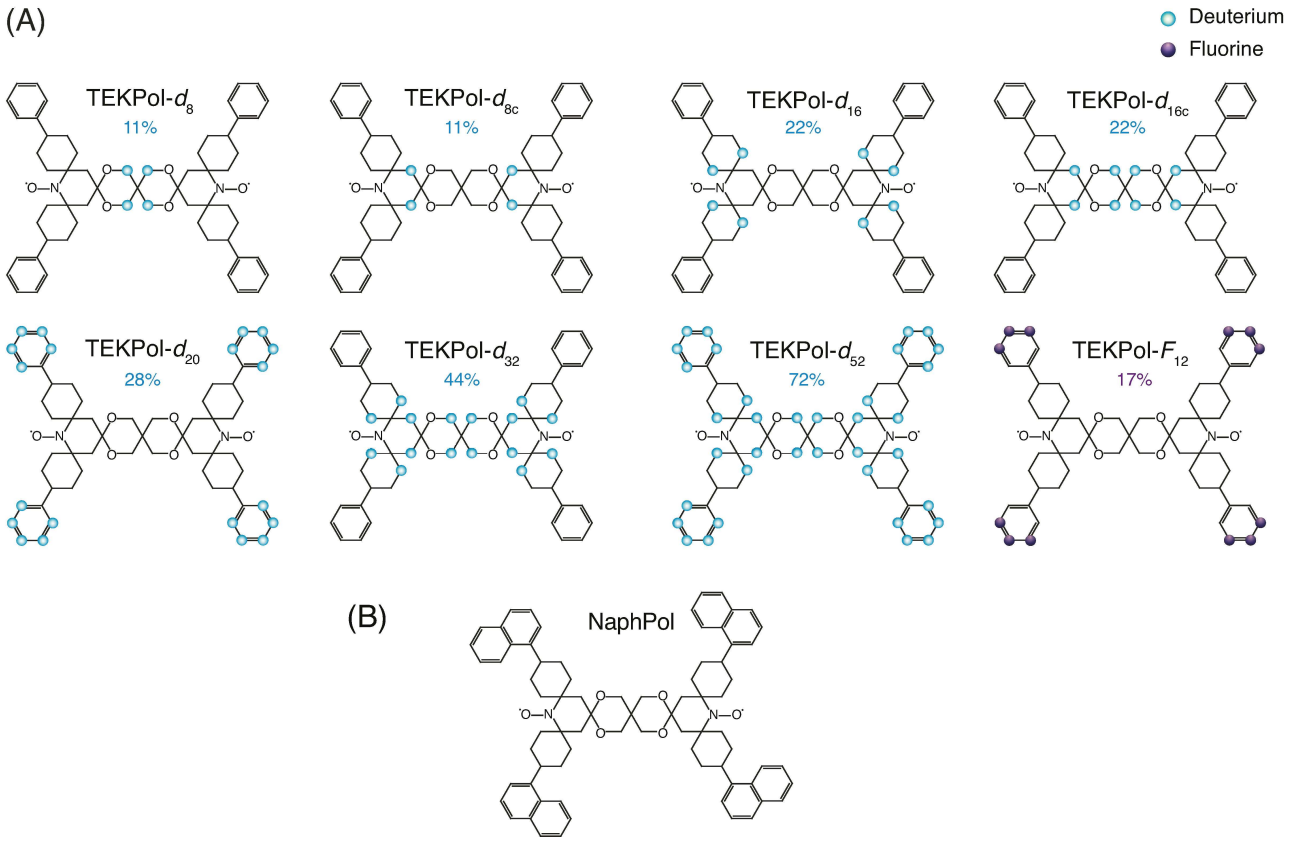

Figure 1. Molecular structures of the newly synthesized biradicals studied here. A) Structures of deuterated TEKPol (-d_8, -d_{8c}, -d_{16}, -d_{16c}, -d_{20}, -d_{32} and -d_{52}) and fluorinated TEKPol (-F_{12}) biradicals. The subscript d_n or F_n indicates the number of protons that are replaced by deuterons (blue) or fluorine (purple), respectively. The color code indicates the deuterated and fluorinated carbons. Deprotonation levels are indicated. B) Structure of a new biradical NaphPol. See Supporting Information for details on synthesis and characterization.

positions. Detailed synthetic protocols are provided in the Supporting Information.

Figure 2 and Table S1 show the experimental ^{1}H DNP enhancements (ε) and build-up times (T_B) measured with 16 mM solutions of the TEKPol-d_n/F_{12} biradicals in fully protonated 1,1,2,2-tetrachloroethane (TCE) and 9:1 TCE-d_2:TCE (hereafter referred to as 90 % TCE-d_2) solutions at 100 K. In both solvent environments, the ^{1}H DNP enhancements decreased with higher biradical deuteration levels whereas the DNP build-up times increased concomitantly (Figure 2B and C). For example, comparing TEKPol and TEKPol-d_{52} in protonated TCE, the ε and T_B change from 202 and 3.08 s, to 137 and 7.52 s, respectively, whereas in 90 % TCE-d_2 the corresponding changes are from 124 and 3.1 s to 85 and 10.2 s.

At first glance, this observation is directly contrary to previous results with bTbK and TOTAPOL, where the enhancements were found to increase with deuteration and positively correlate with increasing electron longitudinal (T_{1e}) relaxation times.[28a] However, both bTbK and TOTAPOL contain four methyl groups close to the nitroxide group, which are known to reduce electron relaxation times and saturation factors.[6,20,29] Methyl groups are also known to act as nuclear relaxation sinks.[20,28a] Consequently, the largest enhancement gains were obtained when the methyl groups were deuterated.[28a] Notably, Geiger et al. showed that selective deuteration of the methyl groups in TOTAPOL led to a factor two increase in DNP enhancements. Any additional deuteration only led to a decrease in the enhancement, which was suggested to be due to the presence of fewer protons to "pickup" the hyperpolarization.[28b]

On the other hand, TEKPol is a rigid biradical that does not contain any methyl groups, and in fact, the replacement of the methyl groups in bTbK with bulky cyclohexyl-phenyl substituents, to improve the electron saturation factors, was key to the development of TEKPol.[6] Here Q-band electron spin relaxation times are probed through measurements of the inversion-recovery (T_{ir}) and phase memory times (T_m) in 16 mM solutions. In the following we refer to these measured values as T_{1e} and T_{2e}, for simplicity. We find the Q-band electron spin relaxation times are largely unchanged across the TEKPol series studied here, except in the case of TEKPol-F_{12} where the electron spin relaxation times are significantly lower in comparison to the TEKPol-d_n (Figure S6, Table S4). Based on the model proposed by Prisco et al., an increase in T_B corresponds to a decrease in the polarization transfer coefficient at the spin diffusion barrier interface (k_{DNP}).[22a] This suggests that k_{DNP} decreases with biradical deprotonation. The reduction in T_B and the apparent increase in k_{DNP} with TEKPol-F_{12} (Table S3) is possibly caused by faster paramagnetic relaxation of the nearby proton spins due to its shorter electron relaxation times (Table S4). Overall, the decreasing k_{DNP} with increasing deprotonation supports the idea that the bulk enhancements in these solutions are being limited by the polarization transfer efficiency between protons across the spin diffusion barrier interface.[22a] Therefore, our observations can be explained to occur likely due to two effects: (i) the

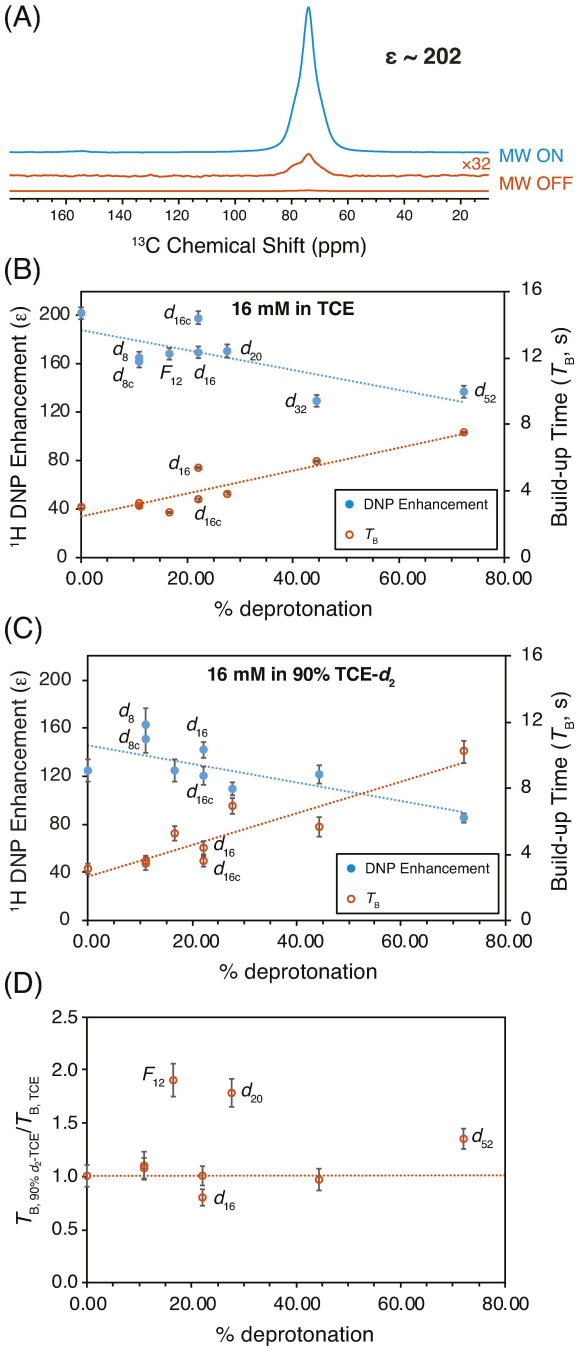

Figure 2. A) ^{1}H→^{13}C cross polarization (CP) MAS spectra under microwave on (blue) and off (orange) conditions of a solution of 16 mM TEKPol in 1,1,2,2-tetrachloroethane (TCE); the ^{13}C signal of the TCE solvent is observed at ca. 74 ppm. Plots showing ^{1}H DNP enhancements (ε) and ^{1}H DNP build-up times (T_B) as a function of percent deprotonation of the TEKPol molecule with 16 mM solutions of TEKPol-d_n/-F_{12} in fully protonated TCE (B) and 90% TCE-d_2 (C) (9:1 TCE-d_2:TCE). ε is defined as the ratio of the integrated signal intensities under microwave on and off conditions (I_{on}/I_{off}). In all cases, ^{1}H DNP enhancements were measured by recording ^{13}C CPMAS spectra of the kind shown in (A) (details in Supporting Information; Tables S1 and S2). D) Plot showing the ratio of the ^{1}H DNP build-up times in 90% TCE-d_2 and protonated TCE. Dotted lines in (B) and (C) show linear regressions and the dotted line in (D) is a guide for the eye.

reduction in the number of strongly hyperfine coupled protons in the vicinity of the radical, and (ii) the availability of fewer protons to transport the hyperpolarization away from the biradical.

Comparison of the measurements in fully protonated and 90 % TCE-d_2 solutions shows that the ^{1}H DNP enhancements decrease on average by ca. 25 % (Figure 2, Table S1) in 90 % TCE-d_2; this observation can be explained by the near-optimal proton concentration of fully protonated TCE.[30] The decrease in enhancement in 90 % TCE-d_2 is due to a reduction in spin diffusion rates in the bulk solvent at lower proton concentrations.[22a] On the other hand, T_B was found to be similar for most of the radicals in protonated and 90 % TCE-d_2, except for three cases: TEKPol-F_{12}, -d_{20}, and -d_{52} (Figure 2D). In other words, the DNP efficiency of these three biradicals in 90 % TCE-d_2 is severely limited by a slow transfer of polarization across the spin diffusion barrier interface, more so than the other biradicals. Interestingly, the only commonality between TEKPol-F_{12}, -d_{20}, and -d_{52} is that their structures are all deprotonated in the phenyl groups (Figure 1). This observation strongly suggests that the phenyl groups play a critical role in transporting the hyperpolarization into the bulk, which is especially visible in 90 % TCE-d_2, in agreement with previous predictions.[31]

To quantify the effects of depolarization and quenching on the overall sensitivity of the radicals studied here, we recorded quantitative ^{1}H→^{13}C cross polarization (CP) spectra to measure the contribution factor (θ) and overall sensitivity gains in comparison to the pure solvent (Figure 3; see Experimental and Table S2 in the Supporting Information for details).[19,20] The changes in θ observed here (Figure 3A) cannot be explained by electron T_{1e}[32] or by differences in relative g-tensor variations[33] which are both similar across the series of deuterated radicals here (Figures S4 and S6). It is known that cross effect events under microwave off conditions lead to depolarization, which should be propagated to the bulk similar to the hyperpolarization under microwave on conditions. Consequently, the measured θ values are inversely correlated to the ^{1}H DNP enhancements (Figure 3A). The overall sensitivity enhancement (Σ), which is proportional to ε, θ and $T_B^{-1/2}$, is highest for the radicals which are minimally deprotonated (namely, TEKPol-d_0, -d_8, -d_{8c} and -F_{12}), whereas Σ reduces sharply with increasing radical deuteration (Figure 3B). This observation clearly establishes that TEKPol radicals with minimal to no deuteration provide the best DNP efficiency.

A closer inspection of the trends in ε, T_B and θ reveal deviations that cannot be explained by the observations made so far, and which suggest that additional factors may also be at play. For example, comparing TEKPol ($\varepsilon = 202 \pm 7$) with TEKPol-d_8/-d_{8c} ($\varepsilon = 165 \pm 5$ and 162 ± 5, respectively) the enhancement is reduced by 25 % while the T_B are similar (Figure 2, Table S1). Also, a group of radicals (TEKPol-d_8, -d_{8c}, -d_{16}, -d_{20} and -F_{12}) which have similar enhancements of around 165 show a variation of θ from 0.37–0.45. These variations might be due to experimental errors, but they could also be due to other mechanisms. The sources of the variations around the main trends observed and discussed above will be the subject of future study.

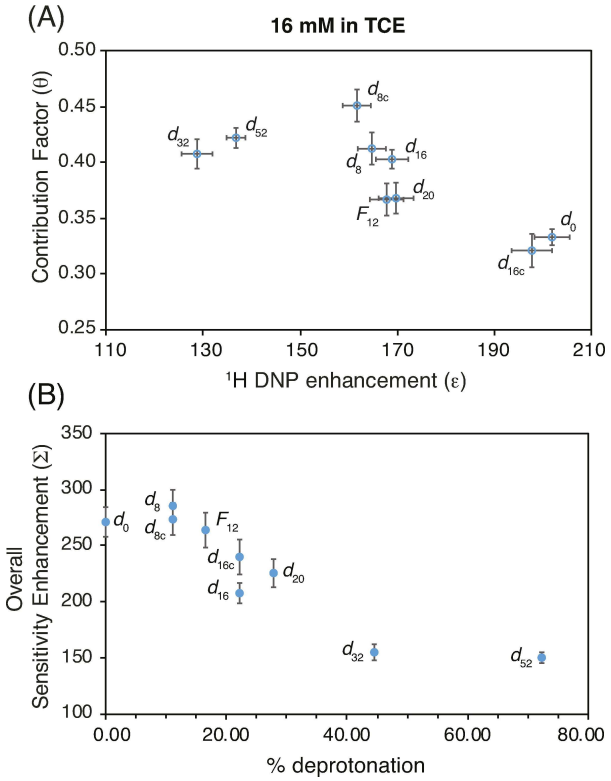

Figure 3. Plots showing (A) contribution factor (θ) and (B) overall sensitivity enhancement (Σ) of 16 mM solutions of TEKPol-d_n/-F_{12} in TCE. Details in Supporting Information (see Experimental and Table S2).

Recent advances in the theoretical description of DNP processes and numerical simulations have furthered the understanding of parameters that determine DNP efficiency.[31,33–35] To explain the experimental trends, we calculated the electron-nuclear hyperfine couplings in TEKPol using density functional theory (DFT). DFT shows that the electron spin density is delocalized over the cyclohexyl group leading to sizeable isotropic hyperfine couplings, up to 2.7 MHz, far away from the nitroxide group (Figure 4A).

Then, using the DFT-derived hyperfine couplings we calculated the polarization and T_B under microwave on and off conditions as previously described by Perras et al.[34] The results are shown in Figure S9 and Table S7. Calculations were performed for all the radicals shown in Figure 1, including TEKPol-d_{20c} and -d_{72} (see Figure S8) that were not synthesized and studied experimentally. With the inclusion of the hyperfine couplings from DFT into the calculations, we see a strong agreement between the experimental and the calculated ε and T_B values (Figure 4B, C). Note that the experimental DNP enhancements are compared with the calculated polarization $I_{on}/I_{Boltzmann}$, as suggested previously.[34] The trend in T_B is reproduced precisely in the calculations, and the agreement between the predicted and experimental T_B values can be further improved by varying

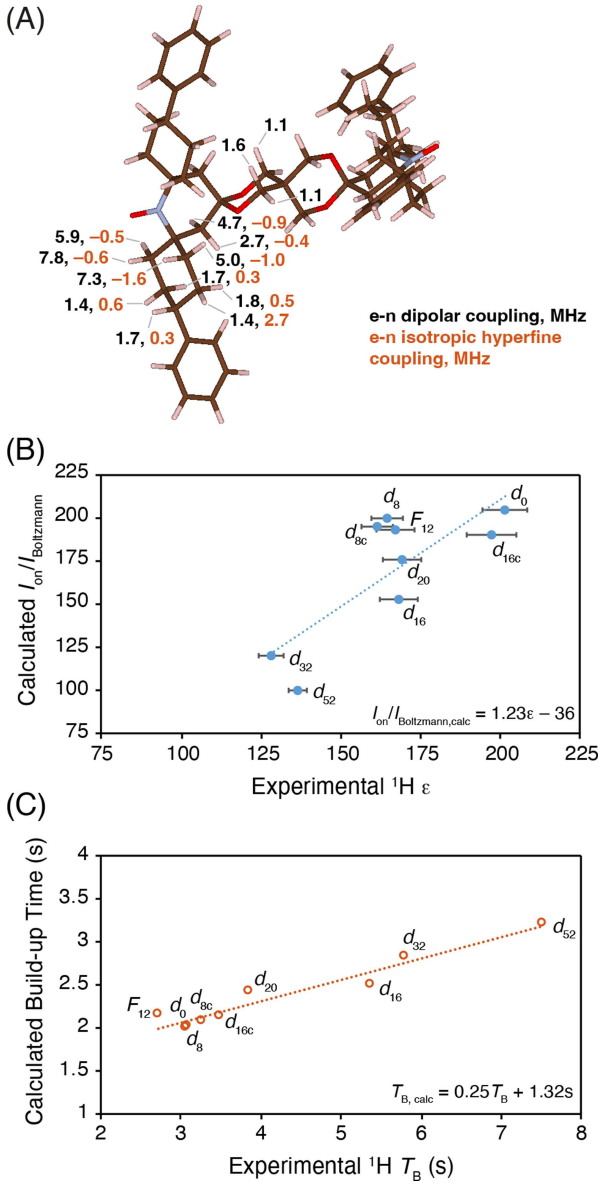

Figure 4. A) DFT-optimized structure of TEKPol using the single crystal X-ray structure as input.[6] The dipolar couplings (black) shown correspond to the largest principal component of the anisotropic hyperfine coupling tensor. The protons in the linker have weak isotropic couplings (<20 kHz) that are not shown. The calculated values are listed in Table S6. Comparison of calculated and experimental ^{1}H DNP enhancements (B) and build-up times (T_B) (C) in TCE for all the radicals shown in Figure 1. Experimental enhancements are compared with $I_{on}/I_{Boltzmann}$ from the calculations as suggested previously.[34] The equations corresponding to the best-fit lines are shown in the plots. Error bars for experimental T_B are small (Table S1), and are not shown for clarity.

the T_1 of the protons nearest and farthest from the radical (see Supporting Information, Table S8).[34] Note that if hyperfine couplings are used that are evaluated based on the electron-nuclear distances alone,[34] relatively poor agreement is found, as the predicted enhancement decreases and T_B increases much more sharply when the protons nearest to the nitroxide are removed than seen in experiment (Figure S9).

We find that when the protons with the largest predicted isotropic hyperfine couplings are removed (in TEKPol-d_{20c}), the predicted enhancements decrease and build-up times increase sharply. Similarly, removing the nearest protons in the cyclohexyl group (TEKPol-d_{16}), which are predicted to have large anisotropic hyperfine couplings, also increases the build-up time sharply (Figure S9B). Given that these cyclohexyl protons are predicted to have the strongest hyperfine couplings (isotropic/anisotropic), it is not surprising that the phenyl groups are the preferred pathway for the polarization transfer, as seen in the experiments. Given that extensive deuteration of the linker slightly increases the build-up time, it is possible the polarization may be propagated to the solvent via these protons to a lesser extent.

Taken together, our findings clearly show that DNP enhancements are indeed limited by electron-nuclear hyperfine couplings and ^{1}H-^{1}H spin diffusion in the vicinity of the radical. While the first polarization step relies on strong hyperfine couplings to the surrounding protons, this polarization must be transported rapidly to the bulk using ^{1}H-^{1}H dipolar couplings. Our observations also highlight the importance of accurate electron-nuclear hyperfine couplings in DNP simulations, and that the key protons in the polarization transfer pathway may not always be those closest to the nitroxide group.

Finally to exploit our new understanding of the preferred polarization transfer pathway in TEKPol, we designed a new biradical, dubbed NaphPol, in which the phenyl groups of TEKPol are replaced with naphthyl groups (Figure 1B). Interestingly, for NaphPol the ^{1}H ε and θ increase from 202 to 249 and 0.33 to 0.38, respectively, in comparison to TEKPol, while the T_B only increases slightly, to 3.6 s. Consequently, the overall sensitivity enhancement (Σ) improves significantly from 265 for TEKPol to 350 for NaphPol (Table 1), making NaphPol the best performing biradical in organic solvents to date.

We remark that the measured electron spin relaxation times of NaphPol differ slightly from TEKPol (Table S5), resulting in a larger saturation factor for NaphPol ($T_{1e}T_{2e}$ = 622 μs^2) in comparison to TEKPol ($T_{1e}T_{2e}$ = 540 μs^2), which may slightly increase T_B. Indeed, bulky groups and higher molecular weight are known to increase the electronic saturation factor,[6] and should also be beneficial for DNP enhancements,[20] but the increase in $T_{1e}T_{2e}$ is unlikely to fully explain the 25 % increase in enhancement with NaphPol. For example, TEKPol2 was previously shown to have a 50 % larger $T_{1e}T_{2e}$ than TEKPol, but the DNP enhancement increased by only ≈8 %.[20] This result strongly

Table 1: Comparison of measured DNP properties of NaphPol and TEKPol.

Radicals	^{1}H ε	^{1}H T_B	θ	Σ
TEKPol	202 ± 7	3.1	0.33 ± 0.01	265 ± 13
NaphPol	249 ± 4	3.6	0.38 ± 0.01	350 ± 9

validates the insights gained from the deprotonated TEKPol series and provides a new criterion for designing biradicals for DNP.

Conclusion

In summary, a series of deuterated and fluorinated TEKPol biradicals were synthesized and their cross-effect DNP efficiency was studied at 9.4 T and 100 K. The ^{1}H DNP enhancements were found to decrease and build-up times were found to increase with increasing biradical deuteration in both protonated and 90 % TCE-d_2 solvent environments. The increase in T_B with biradical deuteration corresponds to a decrease in k_{DNP}, where the bulk DNP enhancements are limited by polarization transfer across the spin diffusion barrier interface. This effect occurs because of two reasons: first, the initial polarization transfer step from the electron to nuclear spins on the radical depends strongly on the strength of the hyperfine couplings. Therefore, when strongly hyperfine coupled protons are removed, the bulk is more slowly hyperpolarized. Second, protons on the biradical also play a critical role in transporting the hyperpolarization into the bulk. Notably, especially with 90 % TCE-d_2 solutions, it was found that the phenyl group protons play a crucial role in the transfer of hyperpolarization into the bulk. This observation is also relevant in the context of fast MAS DNP experiments when highly deuterated solutions can be used to facilitate ^{1}H detection. Based on the new understanding of the preferred polarization transfer pathway in TEKPol, a new biradical was designed, dubbed NaphPol, in which the phenyl groups of TEKPol are replaced with naphthyl groups, and which was shown to yield a 30 % increase in overall sensitivity.

Acknowledgements

We are grateful to Manuel Cordova (EPFL) for help in compiling the numerical DNP simulation package. This work was supported by Swiss National Science Foundation Grant No. 200020_212046, EU H2020-INFRAIA Grant No. 101008500, and by an H2020 Marie Skłodowska-Curie Individual fellowship (grant number 101024369) (AV). Open Access funding provided by École Polytechnique Fédérale de Lausanne.

Conflict of Interest

The authors declare no conflict of interest.

Data Availability Statement

The data that support the findings of this study are openly available at the following link (https://zenodo.org/record/7955264). The data and code are available under the CC-BY-4.0 (Creative Commons Attribution 4.0 International) license.

Keywords: Hyperpolarization · dynamic nuclear polarization · NMR spectroscopy · polarizing agents

[1] a) A. S. Lilly Thankamony, J. J. Wittmann, M. Kaushik, B. Corzilius, *Prog. Nucl. Magn. Reson. Spectrosc.* **2017**, *102–103*, 120; b) A. J. Rossini, A. Zagdoun, M. Lelli, A. Lesage, C. Copéret, L. Emsley, *Acc. Chem. Res.* **2013**, *46*, 1942; c) T. Maly, G. T. Debelouchina, V. S. Bajaj, K. N. Hu, C. G. Joo, M. L. Mak-Jurkauskas, J. R. Sirigiri, P. C. van der Wel, J. Herzfeld, R. J. Temkin, R. G. Griffin, *J. Chem. Phys.* **2008**, *128*, 052211; d) Q. Z. Ni, E. Daviso, T. V. Can, E. Markhasin, S. K. Jawla, T. M. Swager, R. J. Temkin, J. Herzfeld, R. G. Griffin, *Acc. Chem. Res.* **2013**, *46*, 1933.

[2] a) P. Berruyer, S. Björgvinsdóttir, A. Bertarello, G. Stevanato, Y. Rao, G. Karthikeyan, G. Casano, O. Ouari, M. Lelli, C. Reiter, F. Engelke, L. Emsley, *J. Phys. Chem. Lett.* **2020**, *11*, 8386; b) D. Wisser, G. Karthikeyan, A. Lund, G. Casano, H. Karoui, M. Yulikov, G. Menzildjian, A. C. Pinon, A. Purea, F. Engelke, S. R. Chaudhari, D. Kubicki, A. J. Rossini, I. B. Moroz, D. Gajan, C. Copéret, G. Jeschke, M. Lelli, L. Emsley, A. Lesage, O. Ouari, *J. Am. Chem. Soc.* **2018**, *140*, 13340; c) G. Mathies, M. A. Caporini, V. K. Michaelis, Y. P. Liu, K. N. Hu, D. Mance, J. L. Zweier, M. Rosay, M. Baldus, R. G. Griffin, *Angew. Chem. Int. Ed.* **2015**, *54*, 11770.

[3] A. Lesage, M. Lelli, D. Gajan, M. A. Caporini, V. Vitzthum, P. Mieville, J. Alauzun, A. Roussey, C. Thieuleux, A. Mehdi, G. Bodenhausen, C. Copéret, L. Emsley, *J. Am. Chem. Soc.* **2010**, *132*, 15459.

[4] D. A. Hall, D. C. Maus, G. J. Gerfen, S. J. Inati, L. R. Becerra, F. W. Dahlquist, R. G. Griffin, *Science* **1997**, *276*, 930.

[5] a) K. N. Hu, H. H. Yu, T. M. Swager, R. G. Griffin, *J. Am. Chem. Soc.* **2004**, *126*, 10844; b) C. S. Song, K. N. Hu, C. G. Joo, T. M. Swager, R. G. Griffin, *J. Am. Chem. Soc.* **2006**, *128*, 11385.

[6] A. Zagdoun, G. Casano, O. Ouari, M. Schwarzwälder, A. J. Rossini, F. Aussenac, M. Yulikov, G. Jeschke, C. Copéret, A. Lesage, P. Tordo, L. Emsley, *J. Am. Chem. Soc.* **2013**, *135*, 12790.

[7] C. Sauvée, M. Rosay, G. Casano, F. Aussenac, R. T. Weber, O. Ouari, P. Tordo, *Angew. Chem. Int. Ed.* **2013**, *52*, 10858.

[8] G. Stevanato, G. Casano, D. J. Kubicki, Y. Rao, L. Esteban Hofer, G. Menzildjian, H. Karoui, D. Siri, M. Cordova, M. Yulikov, G. Jeschke, M. Lelli, A. Lesage, O. Ouari, L. Emsley, *J. Am. Chem. Soc.* **2020**, *142*, 16587.

[9] a) F. Mentink-Vigier, I. Marin-Montesinos, A. P. Jagtap, T. Halbritter, J. van Tol, S. Hediger, D. Lee, S. T. Sigurdsson, G. De Paepe, *J. Am. Chem. Soc.* **2018**, *140*, 11013; b) R. Harrabi, T. Halbritter, F. Aussenac, O. Dakhlaoui, J. van Tol, K. K. Damodaran, D. Lee, S. Paul, S. Hediger, F. Mentink-Vigier, S. T. Sigurdsson, G. De Paepe, *Angew. Chem. Int. Ed.* **2022**, *61*, e202114103.

[10] A. Lund, G. Casano, G. Menzildjian, M. Kaushik, G. Stevanato, M. Yulikov, R. Jabbour, D. Wisser, M. Renom-Carrasco, C. Thieuleux, F. Bernada, H. Karoui, D. Siri, M. Rosay, I. V. Sergeyev, D. Gajan, M. Lelli, L. Emsley, O. Ouari, A. Lesage, *Chem. Sci.* **2020**, *11*, 2810.

[11] a) C. F. Hwang, D. A. Hill, *Phys. Rev. Lett.* **1967**, *18*, 110; b) C. F. Hwang, D. A. Hill, *Phys. Rev. Lett.* **1967**, *19*, 1011.

[12] a) M. K. Kiesewetter, B. Corzilius, A. A. Smith, R. G. Griffin, T. M. Swager, *J. Am. Chem. Soc.* **2012**, *134*, 4537; b) F. Mentink-Vigier, *Phys. Chem. Chem. Phys.* **2020**, *22*, 3643; c) Y. Matsuki, T. Maly, O. Ouari, H. Karoui, F. Le Moigne, E.

Rizzato, S. Lyubenova, J. Herzfeld, T. Prisner, P. Tordo, R. G. Griffin, *Angew. Chem. Int. Ed.* **2009**, *48*, 4996.
[13] A. Zagdoun, G. Casano, O. Ouari, G. Lapadula, A. J. Rossini, M. Lelli, M. Baffert, D. Gajan, L. Veyre, W. E. Maas, M. Rosay, R. T. Weber, C. Thieuleux, C. Coperet, A. Lesage, P. Tordo, L. Emsley, *J. Am. Chem. Soc.* **2012**, *134*, 2284.
[14] A. Equbal, K. Tagami, S. Han, *Phys. Chem. Chem. Phys.* **2020**, *22*, 13569.
[15] G. Menzildjian, A. Lund, M. Yulikov, D. Gajan, L. Niccoli, G. Karthikeyan, G. Casano, G. Jeschke, O. Ouari, M. Lelli, A. Lesage, *J. Phys. Chem. B* **2021**, *125*, 13329.
[16] F. Mentink-Vigier, G. Mathies, Y. P. Liu, A. L. Barra, M. A. Caporini, D. Lee, S. Hediger, R. G. Griffin, G. De Paepe, *Chem. Sci.* **2017**, *8*, 8150.
[17] Y. X. Li, A. Equbal, K. Tagami, S. Han, *Chem. Commun.* **2019**, *55*, 7591.
[18] a) K. R. Thurber, R. Tycko, *J. Chem. Phys.* **2012**, *137*, 084508; b) F. Mentink-Vigier, S. Paul, D. Lee, A. Feintuch, S. Hediger, S. Vega, G. De Paepe, *Phys. Chem. Chem. Phys.* **2015**, *17*, 21824.
[19] A. J. Rossini, A. Zagdoun, M. Lelli, D. Gajan, F. Rascon, M. Rosay, W. E. Maas, C. Coperet, A. Lesage, L. Emsley, *Chem. Sci.* **2012**, *3*, 108.
[20] D. J. Kubicki, G. Casano, M. Schwarzwalder, S. Abel, C. Sauvee, K. Ganesan, M. Yulikov, A. J. Rossini, G. Jeschke, C. Coperet, A. Lesage, P. Tordo, O. Ouari, L. Emsley, *Chem. Sci.* **2016**, *7*, 550.
[21] a) A. A. Smith, B. Corzilius, A. B. Barnes, T. Maly, R. G. Griffin, *J. Chem. Phys.* **2012**, *136*, 015101; b) N. Bloembergen, *Physica* **1949**, *15*, 386; c) C. Ramanathan, *Appl. Magn. Reson.* **2008**, *34*, 409.
[22] a) N. A. Prisco, A. C. Pinon, L. Emsley, B. F. Chmelka, *Phys. Chem. Chem. Phys.* **2021**, *23*, 1006; b) A. C. Pinon, J. Schlagnitweit, P. Berruyer, A. J. Rossini, M. Lelli, E. Socie, M. X. Tang, T. Pham, A. Lesage, S. Schantz, L. Emsley, *J. Phys. Chem. C* **2017**, *121*, 15993.
[23] J. P. Wolfe, *Phys. Rev. Lett.* **1973**, *31*, 907.
[24] K. O. Tan, M. Mardini, C. Yang, J. H. Ardenkjwr-Larsen, R. G. Griffin, *Sci. Adv.* **2019**, *5*, eaax2743.
[25] a) Q. Stern, S. F. Cousin, F. Mentink-Vigier, A. C. Pinon, S. J. Elliott, O. Cala, S. Jannin, *Sci. Adv.* **2021**, *7*, eabf5735; b) D. Guarin, D. Carnevale, M. Baudin, P. Pelupessy, D. Abergel, G. Bodenhausen, *J. Phys. Chem. Lett.* **2022**, *13*, 175.
[26] a) K. O. Tan, L. Yang, M. Mardini, C. Boon Cheong, B. Driesschaert, M. Dinca, R. G. Griffin, *Chem. Eur. J.* **2022**, *28*, e202202556; b) E. P. Saliba, E. L. Sesti, F. J. Scott, B. J. Albert, E. J. Choi, N. Alaniva, C. K. Gao, A. B. Barnes, *J. Am. Chem. Soc.* **2017**, *139*, 6310.
[27] a) L. Delage-Laurin, R. S. Palani, N. Golota, M. Mardini, Y. F. Ouyang, K. O. Tan, T. M. Swager, R. G. Griffin, *J. Am. Chem. Soc.* **2021**, *143*, 20281; b) R. S. Palani, M. Mardini, L. Delage-Laurin, D. Banks, Y. Ouyang, E. Bryerton, J. G. Kempf, T. M. Swager, R. G. Griffin, *J. Phys. Chem. Lett.* **2023**, *14*, 95; c) F. A. Perras, D. F. Flesariu, S. A. Southern, C. Nicolaides, J. D. Bazak, N. M. Washton, T. Trypiniotis, C. P. Constantinides, P. A. Koutentis, *J. Phys. Chem. Lett.* **2022**, *13*, 4000.
[28] a) F. A. Perras, R. R. Reinig, I. I. Slowing, A. D. Sadow, M. Pruski, *Phys. Chem. Chem. Phys.* **2016**, *18*, 65; b) M. A. Geiger, M. Orwick-Rydmark, K. Marker, W. T. Franks, D. Akhmetzyanov, D. Stoppler, M. Zinke, E. Specker, M. Nazare, A. Diehl, B. J. van Rossum, F. Aussenac, T. Prisner, U. Akbey, H. Oschkinat, *Phys. Chem. Chem. Phys.* **2016**, *18*, 30696.
[29] A. Zecevic, G. R. Eaton, S. S. Eaton, M. Lindgren, *Mol. Phys.* **1998**, *95*, 1255.
[30] A. Zagdoun, A. J. Rossini, D. Gajan, A. Bourdolle, O. Ouari, M. Rosay, W. E. Maas, P. Tordo, M. Lelli, L. Emsley, A. Lesage, C. Coperet, *Chem. Commun.* **2012**, *48*, 654.
[31] F. A. Perras, M. Raju, S. L. Carnahan, D. Akbarian, A. C. T. van Duin, A. J. Rossini, M. Pruski, *J. Phys. Chem. Lett.* **2020**, *11*, 5655.
[32] A. Lund, A. Equbal, S. Han, *Phys. Chem. Chem. Phys.* **2018**, *20*, 23976.
[33] Z. H. Gan, *J. Chem. Phys.* **2023**, *158*, 024114.
[34] F. A. Perras, S. L. Carnahan, W. S. Lo, C. J. Ward, J. Q. Yu, W. Y. Huang, A. J. Rossini, *J. Chem. Phys.* **2022**, *156*, 124112.
[35] a) A. Equbal, A. Leavesley, S. K. Jain, S. I. Han, *J. Phys. Chem. Lett.* **2019**, *10*, 548; b) F. Mentink-Vigier, S. Vega, G. De Paepe, *Phys. Chem. Chem. Phys.* **2017**, *19*, 3506; c) D. Mance, P. Gast, M. Huber, M. Baldus, K. L. Ivanov, *J. Chem. Phys.* **2015**, *142*, 234201; d) F. Mentink-Vigier, *J. Magn. Reson.* **2021**, *333*, 107106.

Manuscript received: April 5, 2023
Accepted manuscript online: May 24, 2023
Version of record online: ■■, ■■

Forschungsartikel

NMR Spectroscopy

A. Venkatesh, G. Casano, Y. Rao, F. De Biasi, F. A. Perras, D. J. Kubicki, D. Siri, S. Abel, H. Karoui, M. Yulikov, O. Ouari,* L. Emsley* ——— **e202304844**

Deuterated TEKPol Biradicals and the Spin-Diffusion Barrier in MAS DNP

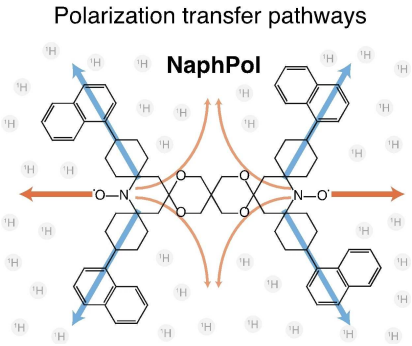

Dynamic nuclear polarization NMR of a series of deuterated and fluorinated TEKPol biradicals allows the elucidation of the hyperpolarization transfer pathway. This knowledge has enabled the design of a new polarization agent, NaphPol, which is the most efficient biradical in organic solvents to date.